Eur. Phys. J. C (2021) 81:664
https://doi.org/10.1140/epjc/s10052-021-09466-1

THE EUROPEAN PHYSICAL JOURNAL C

Regular Article - Theoretical Physics

Probing anomalous quartic $\gamma\gamma\gamma\gamma$ couplings in light-by-light collisions at the CLIC

S.C. İnan[1,a], **A.V. Kisselev**[2,b]

[1] Department of Physics, Sivas Cumhuriyet University, 58140 Sivas, Turkey
[2] Division of Theoretical Physics, A.A. Logunov Institute for High Energy Physics, NRC "Kurchatov Institute", Protvino 142281, Russia

Received: 12 January 2021 / Accepted: 21 July 2021

Abstract The anomalous quartic neutral couplings of the $\gamma\gamma\gamma\gamma$ vertex in a polarized light-by-light scattering of the Compton backscattered photons at the CLIC are examined. Both differential and total cross sections are calculated for e^+e^- collision energies 1500 GeV and 3000 GeV. The helicity of the initial electron beams is taken to be ± 0.8. The unpolarized and SM cross sections for the same values of helicities are also estimated. The 95% C.L. exclusion limits on two anomalous photon couplings ζ_1 and ζ_2 are calculated. The best bounds on these couplings are found to be 6.85×10^{-16} GeV^{-4} and 1.43×10^{-15} GeV^{-4}, respectively. The results are compared with the exclusion bounds obtained previously for the LHC and HL-LHC. It is shown that the light-by-light scattering at the CLIC, especially the polarized, has a greater potential to search for the anomalous quartic neutral couplings of the $\gamma\gamma\gamma\gamma$ vertex.

1 Introduction

In the Standard Model (SM), the trilinear gauge couplings (TGCs) [1,2] and quartic gauge couplings (QGCs) [3–6] are completely defined by the non-Abelian $SU(2)_L \times U(1)_Y$ gauge symmetry. These couplings have been accurately tested by experiments. A possible deviation from the electroweak predictions can give us important information on probable physics beyond the SM.

Anomalous TGCs and QGCs can be studied in a model independent way in the framework of the effective field theory (EFT) via Lagrangian [7–10]

$$\mathcal{L}_{\rm eff} = \mathcal{L}_{\rm SM} + \mathcal{L}_{(6)} + \mathcal{L}_{(8)}. \tag{1}$$

The Lagrangian $\mathcal{L}_{(6)}$ contains dimension-6 operators. It generates an anomalous contribution to the TGCs and QGCs. Let us underline that the lowest dimension operators that modify the quartic gauge interactions without exhibiting two or three weak gauge boson vertices are dimension-8. The Lagrangian $\mathcal{L}_{(8)}$ is a sum of dimension-8 genuine operators,

$$\mathcal{L}_{(8)} = \sum_i \frac{c_i}{\Lambda^4} \mathcal{O}_i^{(8)}, \tag{2}$$

where Λ is a mass-dimension scale associated with new physics, and c_i are dimensionless constants. This Lagrangian induces anomalous deviation to the QGCs. It is assumed that the new interaction respects the local $SU(2)_L \times U(1)_Y$ symmetry which is broken spontaneously by the vacuum expectation value of the Higgs field Φ. CP invariance is also imposed. It means that $\mathcal{L}_{(8)}$ is invariant under the full gauge symmetry. As a result, the electroweak gauge bosons can appear in the operators $\mathcal{O}_i^{(8)}$ only from covariant derivatives of the Higgs doublet $D_\mu\Phi$ or from the field strengths $B_{\mu\nu}$, $W^a_{\mu\nu}$.

There are three classes of dimension-8 operators. The first one contains just $D_\mu\Phi$. It leads to non-standard quartic couplings of massive vector bosons, $W^+W^-W^+W^-$, W^+W^-ZZ and $ZZZZ$. The second class contains two $D_\mu\Phi$ and two field strength tensors. The third class has four field strength tensors only. The dimension-8 operators of the last two classes induce the anomalous quartic neutral couplings of the vertices $\gamma\gamma\gamma\gamma, \gamma\gamma\gamma Z, \gamma\gamma ZZ, \gamma ZZZ$, and $ZZZZ$. A complete list of dimension-8 operators which lead to anomalous quartic neutral gauge boson couplings is presented in [11–13]. In particular, the effective Lagrangian of the operators $\mathcal{O}_i^{(8)}$ which contributes to the anomalous quartic couplings of the vertex $\gamma\gamma\gamma\gamma$ looks like

$$\mathcal{L}_{\rm QNGC} = \frac{c_8}{\Lambda^4} B_{\rho\sigma}B^{\rho\sigma}B_{\mu\nu}B^{\mu\nu} + \frac{c_9}{\Lambda^4} W^a_{\rho\sigma}W^{a\rho\sigma}W^b_{\mu\nu}W^{b\mu\nu} + \frac{c_{10}}{\Lambda^4} W^a_{\rho\sigma}W^{b\rho\sigma}W^a_{\mu\nu}W^{b\mu\nu} + \frac{c_{11}}{\Lambda^4} B_{\rho\sigma}B^{\rho\sigma}W^a_{\mu\nu}W^{a\mu\nu}$$

[a] e-mail: sceminan@cumhuriyet.tr
[b] e-mail: alexandre.kisselev@ihep.ru (corresponding author)

Published online: 29 July 2021

$$+\frac{c_{13}}{\Lambda^4}B_{\rho\sigma}B^{\sigma\nu}B_{\nu\mu}B^{\mu\rho}+\frac{c_{14}}{\Lambda^4}W^a_{\rho\sigma}W^{a\sigma\nu}W^b_{\nu\mu}W^{b\mu\rho}$$
$$+\frac{c_{15}}{\Lambda^4}W^a_{\rho\sigma}W^{b\sigma\nu}W^a_{\nu\mu}W^{b\mu\rho}+\frac{c_{16}}{\Lambda^4}B_{\rho\sigma}B^{\sigma\nu}W^a_{\nu\mu}W^{a\mu\rho}, \quad (3)$$

see Eq. (5) below.

The explicit expression for dimension-8 Lagrangian in a broken phase (in which it is expressed in terms of the physical fields $W^{\pm}$, Z and $F_{\mu\nu}$) can be found, for instance, in [12]. We are interested in an effective Lagrangian for the anomalous $\gamma\gamma\gamma\gamma$ couplings. It is given by the formula [12]

$$\mathcal{L}^{\gamma\gamma\gamma\gamma}_{\rm QNGC}=\zeta_1 F_{\mu\nu}F^{\mu\nu}F_{\rho\sigma}F^{\rho\sigma}+\zeta_2 F_{\mu\nu}F^{\nu\rho}F_{\rho\sigma}F^{\sigma\mu}, \quad (4)$$

where

$$\zeta_1=[\,c_w^4c_8+s_w^4c_9+c_w^2s_w^2(c_{10}+c_{11})\,]\Lambda^{-4},$$
$$\zeta_2=[\,c_w^4c_{13}+s_w^4c_{14}+c_w^2s_w^2(c_{15}+c_{16})\,]\Lambda^{-4}. \quad (5)$$

The QGCs are actively studied for a long time. The anomalous $WWZZ$ vertex was probed at the LEP [14–17] (see also [18]) and Tevatron [19] colliders. The L3 Collaboration also searched for the $WWZZ$ couplings [20]. There have been investigations for the $WW\gamma\gamma$ couplings at the LHC in [21–30]. The possibility of measuring the $ZZ\gamma\gamma$ couplings were studied in [21–26], [12] and [31]. Recently, the LHC experimental bounds on QGCs have been presented by the CMS [32] and ATLAS [33] Collaborations. In a number of theoretical papers, search limits for the anomalous vertex $WW\gamma\gamma$ at future electron-proton colliders have been estimated [34–36]. The anomalous QGCs can be also probed at linear e^+e^- colliders [37], in particular, in the $e\gamma$ mode [38,39] ($WW\gamma\gamma$, $ZZ\gamma\gamma$ and $WWZ\gamma$ vertices) or $\gamma\gamma$ mode [40] ($WWWW$, $WWZZ$ and $ZZZZ$ vertices), [41] ($WW\gamma\gamma$ and $ZZ\gamma\gamma$ vertices). Finally, in [42,43] the anomalous quartic couplings of the $ZZ\gamma\gamma$ vertex at the Compact Liner Collider (CLIC) [44,45] have been examined. As one can see, in all these papers the anomalous QGCs with the massive gauge bosons were examined.

The great potential of the CLIC in probing new physics is well-known [46–48]. At the CLIC, it is possible to investigate not only e^+e^- scattering but also $e\gamma$ and $\gamma\gamma$ collisions with real photons. In the present paper, we will examine the possibility of searching for anomalous $\gamma\gamma\gamma\gamma$ couplings in the light-by-light (LBL) scattering with ingoing Compton backscattered (CB) photons at the CLIC. Both unpolarized and polarized initial photons will be considered. The first evidence of the process $\gamma\gamma\to\gamma\gamma$ was observed by the ATLAS and CMS Collaborations in high-energy ultra-peripheral PbPb collisions [49–51]. The LBL collisions at the LHC have been studied in [52,53]. Recently, the LBL scattering at the CLIC induced by axion-like particles has been examined [54,55].

2 Light-by-light scattering in effective field theory

The e^+e^- colliders may operate in $e\gamma$ and $\gamma\gamma$ modes [56,57]. Hard real photon beams at the CLIC can be generated by the laser Compton backscattering. When soft laser photons collide with electron beams, a large flux of photons, with a great amount of the parent electron energy, is produced. Let E_0 and λ_0 be the energy and helicity of the initial laser photon beam, while E_e and λ_e be the energy and helicity of the electron beam before CB. In our calculations, two sets of these helicities, with opposite sign of λ_e, will be considered, namely

$$(\lambda_e^{(1)},\lambda_0^{(1)};\lambda_e^{(2)},\lambda_0^{(2)})=(0.8,1;0.8,1),$$
$$(\lambda_e^{(1)},\lambda_0^{(1)};\lambda_e^{(2)},\lambda_0^{(2)})=(-0.8,1;-0.8,1), \quad (6)$$

where the superscripts 1 and 2 enumerate the beams. The helicity of the photon with energy E_γ obtained by the Compton backscattering of the laser photons with helicity λ_0 off the electron beam is given by the formula

$$\xi(E_\gamma,\lambda_0)=\frac{\lambda_0(1-2r)[1-x+1/(1-x)]+\lambda_e r\zeta[1+(1-x)(1-2r)^2]}{1-x+1/(1-x)-4r(1-r)-\lambda_e\lambda_0 r\zeta(2r-1)(2-x)}, \quad (7)$$

where $x=E_\gamma/E_e$, $r=x/\zeta(1-x)$, $\zeta=4E_eE_0/m_e^2$, m_e being the electron mass.

The spectrum of the CB photons is defined by the helicities λ_0, λ_e and dimensionless variables x, r, ζ as follows

$$f_{\gamma/e}(x)=\frac{1}{g(\zeta)}\left[1-x+\frac{1}{1-x}-\frac{4x}{\zeta(1-x)}+\frac{4x^2}{\zeta^2(1-x)^2}+\lambda_0\lambda_e r\zeta(1-2r)(2-x)\right], \quad (8)$$

where

$$g(\zeta)=g_1(\zeta)+\lambda_0\lambda_e\,g_2(\zeta), \quad (9)$$
$$g_1(\zeta)=\left(1-\frac{4}{\zeta}-\frac{8}{\zeta^2}\right)\ln(\zeta+1)+\frac{1}{2}+\frac{8}{\zeta}-\frac{1}{2(\zeta+1)^2}, \quad (10)$$
$$g_2(\zeta)=\left(1+\frac{2}{\zeta}\right)\ln(\zeta+1)-\frac{5}{2}+\frac{1}{\zeta+1}-\frac{1}{2(\zeta+1)^2}. \quad (11)$$

The maximum possible value of x is equal to

$$x_{\rm max}=\frac{(E_\gamma)_{\rm max}}{E_e}=\zeta/(1+\zeta). \quad (12)$$

The laser beam energy is chosen to maximize the backscattered photon energy E_γ. This can be achieved if one puts $\zeta\simeq 4.8$, then $x_{\rm max}\simeq 0.83$.

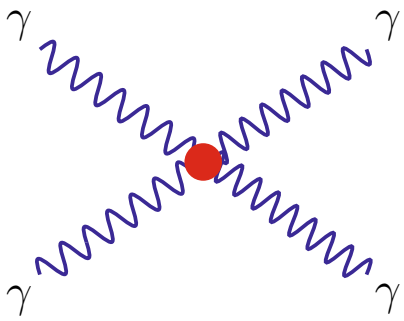

Fig. 1 The diphoton production in the collision of the backscattered photons at the CLIC via anomalous quartic coupling

The LBL scattering of the CB photons happens as shown in Fig. 1. Its differential cross section is expressed in terms of the CB photon spectra, their helicities, and helicity amplitudes [58]

$$\begin{aligned}\frac{d\sigma}{d\cos\theta} &= \frac{1}{128\pi s}\int\limits_{x_{1\min}}^{x_{\max}}\frac{dx_1}{x_1}\,f_{\gamma/e}(x_1)\int\limits_{x_{2\min}}^{x_{\max}}\frac{dx_2}{x_2}\,f_{\gamma/e}(x_2)\\ &\times\Big\{\Big[1+\xi\left(E_\gamma^{(1)},\lambda_0^{(1)}\right)\xi\left(E_\gamma^{(2)},\lambda_0^{(2)}\right)\Big]\\ &\times\left(|M_{++++}|^2+|M_{++--}|^2\right)\\ &+\Big[1-\xi\left(E_\gamma^{(1)},\lambda_0^{(1)}\right)\xi\left(E_\gamma^{(2)},\lambda_0^{(2)}\right)\Big]\\ &\times\left(|M_{+-+-}|^2+|M_{+--+}|^2\right)\Big\},\end{aligned}\tag{13}$$

where $x_1 = E_\gamma^{(1)}/E_e$ and $x_2 = E_\gamma^{(2)}/E_e$ are the energy fractions of the CB photon beams, $x_{1\min} = p_\perp^2/E_e^2$, $x_{2\min} = p_\perp^2/(x_1E_e^2)$, $p_\perp$ is the transverse momentum of the outgoing photons. $\sqrt{s}$ is the center of mass energy of the e^+e^- collider, while $\sqrt{sx_1x_2}$ is the center of mass energy of the backscattered photons. We will apply the cut on the rapidity of the final state photons $|\eta_{\gamma\gamma}| < 2.5$.

The physical potential of linear e^+e^- colliders may be enhanced if the polarized beams are used [59,60]. As will be seen below, it is exactly so in our case. For comparison, similar results for unpolarized electron beams ($\lambda_e^{(1,2)} = 0$) will be also presented. Our calculations have shown that the total cross sections are almost indistinguishable from the SM ones for $\sqrt{s} = 380$ GeV (the first energy stage of the CLIC). That is why, we will focus on the energies $\sqrt{s} = 1500$ GeV (the second energy stage of the CLIC) and $\sqrt{s} = 3000$ GeV (the third energy stage of the CLIC). The expected integrated luminosities for these baseline CLIC energy stages [60] are presented in Table 1.

We have calculated the differential cross sections $d\sigma/dm_{\gamma\gamma}$, where $m_{\gamma\gamma}$ is the invariant mass of the outgoing photons. Each of the amplitudes is a sum of the anomaly and SM terms,

Table 1 The CLIC energy stages and integrated luminosities for the unpolarized and polarized initial electron beams

		L, fb^{-1}		
Stage	$\sqrt{s}$, GeV	$\lambda_e = 0$	$\lambda_e = -0.8$	$\lambda_e = 0.8$
2	1500	2500	2000	500
3	3000	5000	4000	1000

$$M = M_{\text{anom}} + M_{\text{SM}}.\tag{14}$$

As the SM background, we have taken into account both W-loop and fermion-loop contributions

$$M_{\text{SM}} = M_f + M_W.\tag{15}$$

The explicit analytical expressions for the SM helicity amplitudes in the right-hand side of Eq. (13), both for the fermion and W-boson terms, are too long. That is why we do not present them here. They can be found in [54].

The differential cross sections as functions of the photon invariant mass $m_{\gamma\gamma}$ are shown in Figs. 2 and 3. We imposed the cut on the rapidity of the outgoing photons, $|\eta_{\gamma\gamma}| < 2.5$. The left, middle and rights panels of these figures correspond to the electron beam helicities $\lambda_e = 0.8$, $\lambda_e = -0.8$, and $\lambda_e = 0$, respectively. Note that the anomaly amplitude is pure real, while the SM one is mainly imaginary. As a result, the interference contribution to the differential cross section is relatively very small for any values of $m_{\gamma\gamma}$ in the region $m_{\gamma\gamma} > 200$ GeV. If, for instance, $\sqrt{s} = 1500$ GeV, $\lambda_e = 0.8$, $\zeta_1 = 10^{-13}$ GeV^{-4}, $\zeta_2 = 0$, and $m_{\gamma\gamma} = 500$ GeV, the anomaly, SM, and interference terms of the cross section are equal to 3.45×10^{-4} fb/GeV, 5.90×10^{-3} fb/GeV, and 9.05×10^{-5} fb/GeV, respectively. For $\sqrt{s} = 3000$ GeV, the same values of λ_e, $\zeta_{1,2}$, and $m_{\gamma\gamma} = 1000$ GeV we find, correspondingly, 1.05×10^{-2} fb/GeV, 1.64×10^{-3} fb/GeV, and 1.80×10^{-4} fb/GeV.

For both $\sqrt{s}$, and any value of λ_e, the anomaly differential cross sections become to dominate the SM background at about $m_{\gamma\gamma} > 750$ GeV for $\zeta_1 = 10^{-13}$ GeV^{-4}, $\zeta_2 = 0$. For the couplings $\zeta_1 = 0$, $\zeta_2 = 10^{-13}$ GeV^{-4} it takes place in the region $m_{\gamma\gamma} > 960$ GeV. For the same $\sqrt{s}$ and $\zeta_{1,2}$, the differential cross section with $\lambda_e = 0.8$ becomes larger than the differential cross section with the opposite beam helicity $\lambda_e = -0.8$ and unpolarized one, as $m_{\gamma\gamma}$ grows. A possible background with fake photons from decays of π^0, η, and η' is negligible in the signal region.

The leading part of the anomalous cross section is proportional to s^2. However, it does not mean that the unitarity is violated for the region of the anomalous QGCs considered in our paper. As it is shown in [61], the anomalous quartic couplings of the order of 10^{-13} GeV^{-4} do not lead to unitarity violation for the collision energy below 3 TeV.

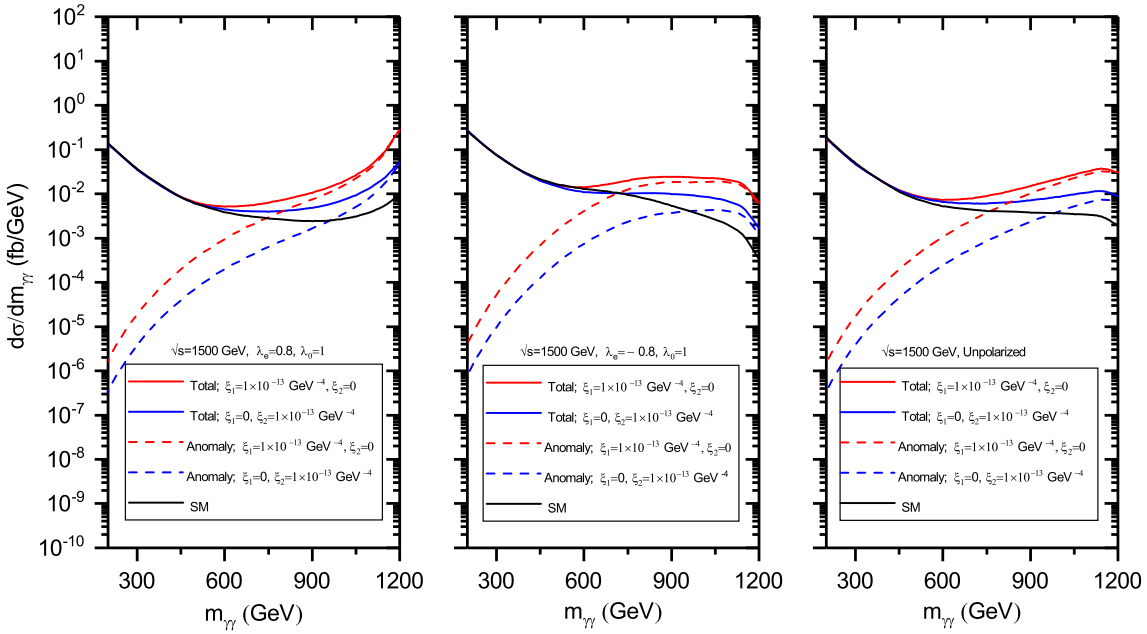

Fig. 2 The differential cross sections for the process $\gamma\gamma \to \gamma\gamma$ as functions of the invariant mass of the outgoing photons for the e^+e^- collider energy $\sqrt{s} = 1500$ GeV. The left, middle and right panels correspond to the electron beam helicity $\lambda_e = 0.8$, -0.8, and 0, respectively. The curves on each plot (from the top downwards) are: the differential cross sections for the coupling sets ($\zeta_1 = 10^{-13}$ GeV^{-4}, $\zeta_2 = 0$) and ($\zeta_1 = 0$, $\zeta_2 = 10^{-13}$ GeV^{-4}), the anomalous contribution for the same coupling values, the SM cross section

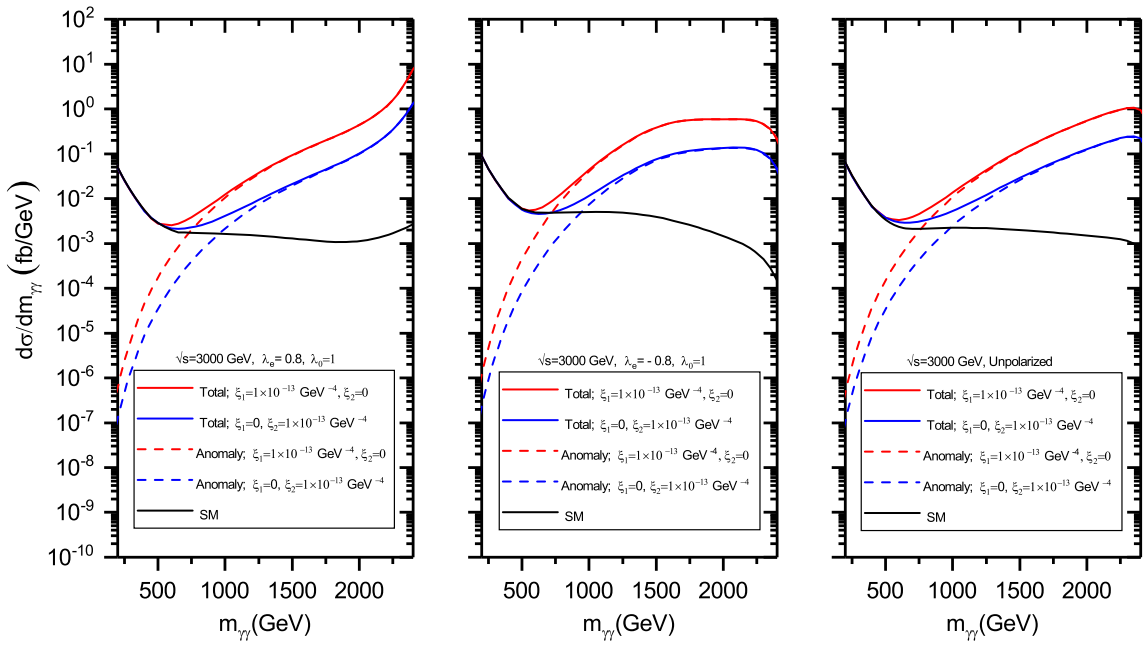

Fig. 3 The same as in Fig. 2, but for the e^+e^- collider energy $\sqrt{s} = 3000$ GeV

The results of our calculations of the total cross sections $\sigma(m_{\gamma\gamma} > m_{\gamma\gamma,\min})$, where $m_{\gamma\gamma,\min}$ is the minimal invariant mass of the outgoing photons, are shown in Figs. 4 and 5. The results are presented for two values of the CLIC energy, and two sets of the couplings ζ_1, ζ_2. The reader can obtain the prediction for any value of the coefficients ζ_1, ζ_2 by simply rescaling the results. For $\sqrt{s} = 1500$ GeV, $\lambda_e = 0.8$, $\zeta_1 = 10^{-13}$ GeV^{-4}, and $\zeta_2 = 0$, the total cross section remains almost unchanged despite increasing $m_{\gamma\gamma,\min}$. A similar tendency takes place for the unpolarized cross section. On the contrary, for $\lambda_e = -0.8$, the total cross sections decrease rapidly, as $m_{\gamma\gamma,\min}$ grows. For $\sqrt{s} = 3000$ GeV

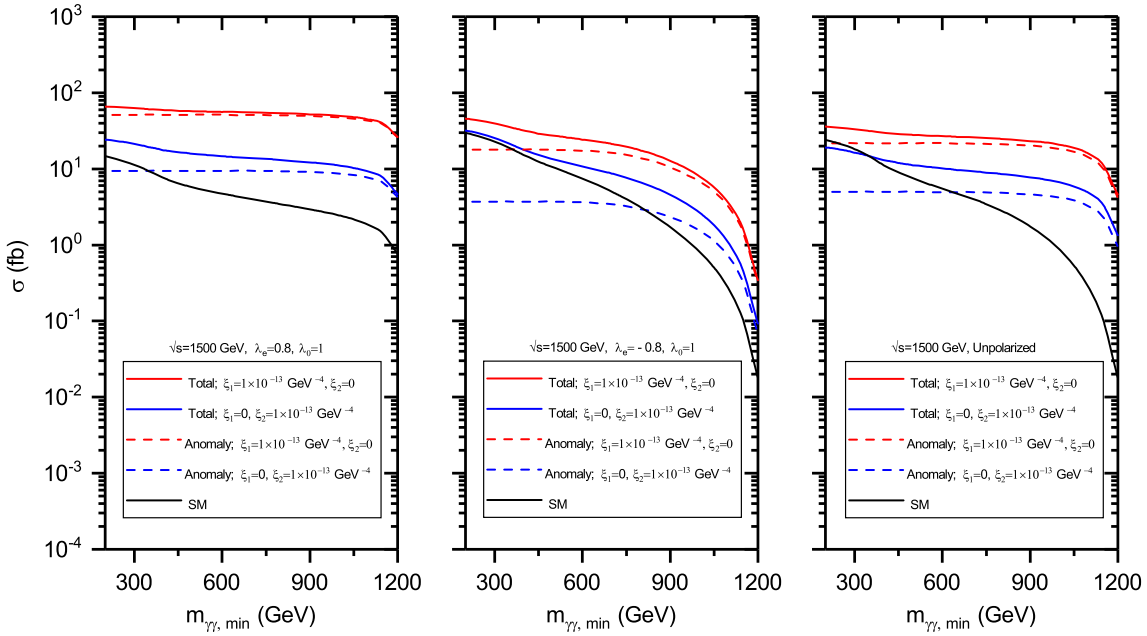

Fig. 4 The total cross sections for the process $\gamma\gamma \to \gamma\gamma$ as functions of the minimal invariant mass of the outgoing photons for the e^+e^- collider energy $\sqrt{s} = 1500$ GeV. The left, middle and right panels correspond to the electron beam helicitiy $\lambda_e = 0.8, -0.8$, and 0, respectively. The curves on each plot (from the top downwards) are: the total cross sections for the coupling sets ($\zeta_1 = 10^{-13}$ GeV^{-4} , $\zeta_2 = 0$) and ($\zeta_1 = 0$, $\zeta_2 = 10^{-13}$ GeV^{-4}), the anomalous contribution for the same coupling values, the SM cross section

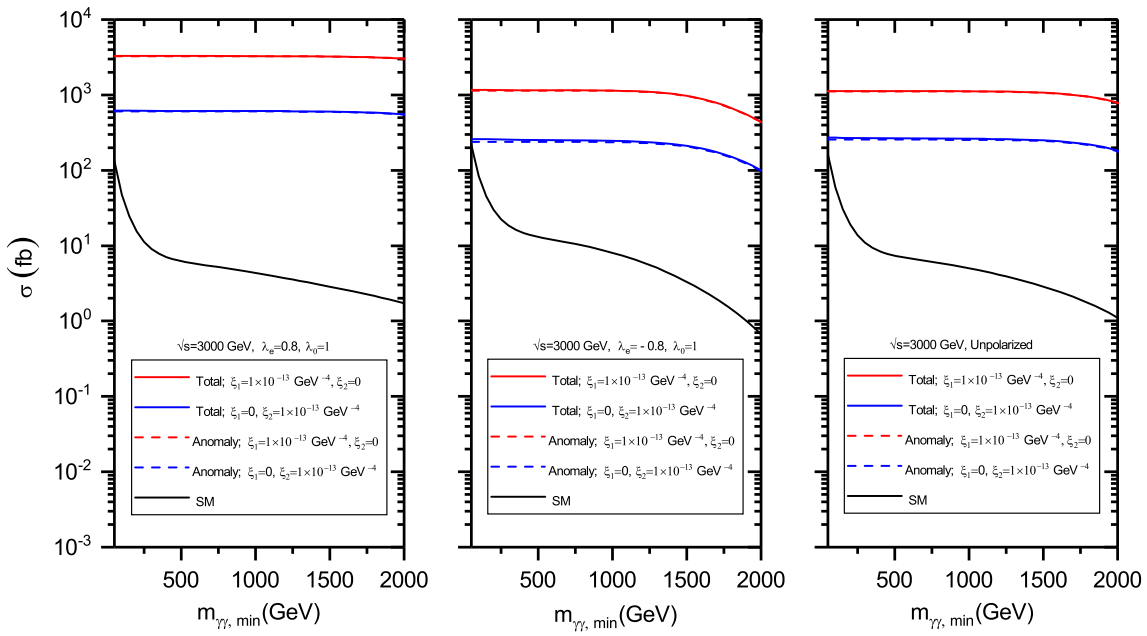

Fig. 5 The same as in Fig. 4, but for the e^+e^- collider energy $\sqrt{s} = 3000$ GeV

the total cross section deviation from the SM gets higher, as $m_{\gamma\gamma,\min}$ increases. $\sigma(m_{\gamma\gamma} > m_{\gamma\gamma,\min})$ with $\lambda_e = 0.8$ and the unpolarized cross section are almost independent of $m_{\gamma\gamma,\min}$, while $\sigma(m_{\gamma\gamma} > m_{\gamma\gamma,\min})$ with $\lambda_e = -0.8$ decreases at large $m_{\gamma\gamma,\min}$. The total cross section with $\lambda_e = 0.8$ is several times large than the total cross section with the opposite beam helicity. Note, however, that for $\lambda_e = 0.8$ the CLIC expected integrated luminosities are four times smaller than those for $\lambda_e = -0.8$, for both values of e^+e^- collision energy, see Table 1.

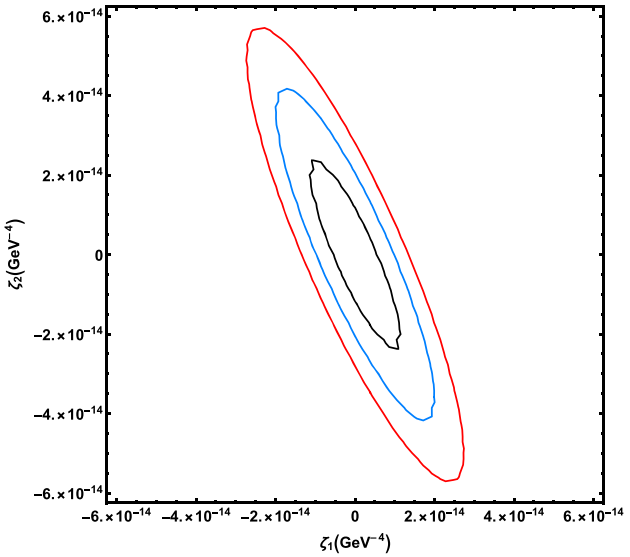

Fig. 6 The 95% C.L. exclusion regions for the couplings ζ_1, ζ_2 for the unpolarized light-by-light scattering at the CLIC with the systematic errors $\delta = 0\%$ (black ellipse), $\delta = 5\%$ (blue ellipse), and $\delta = 10\%$ (red ellipse). The inner regions of the ellipses are inaccessible. The collision energy is $\sqrt{s} = 1500$ GeV, the integrated luminosity is $L = 2500$ fb^{-1}. The cut on the outgoing photon invariant mass $m_{\gamma\gamma} > 1000$ GeV was imposed

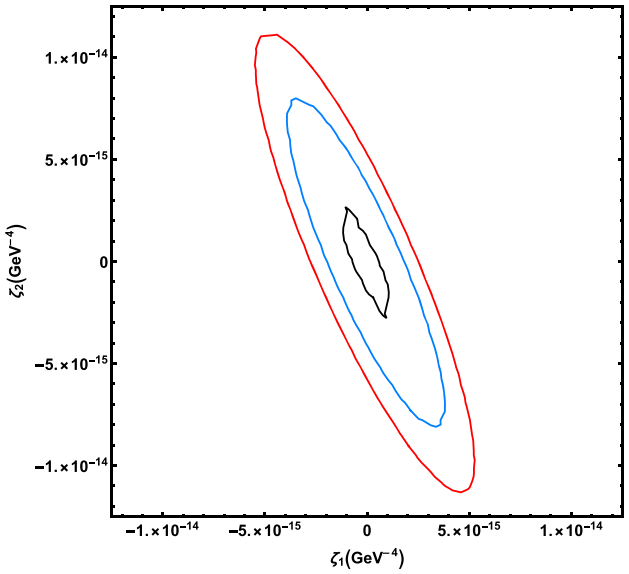

Fig. 7 The same as in Fig. 6, but for $\sqrt{s} = 3000$ GeV and $L = 5000$ fb^{-1}

To calculate the exclusion region, we use the following formula for the exclusion significance [62]

$$S_{\rm excl} = \sqrt{2\left[(s - b\ln\left(\frac{b+s+x}{2b}\right) - \frac{1}{\delta^2}\ln\left(\frac{b-s+x}{2b}\right) - (b+s-x)\left(1+\frac{1}{\delta^2 b}\right)\right]}, \tag{16}$$

with

$$x = \sqrt{(s+b)^2 - 4\delta^2 s b^2/(1+\delta^2 b)}. \tag{17}$$

Here s and b represent the total number of signal and background events, respectively, and δ is the percentage systematic error. In the limit $\delta \to 0$ expression (16) is simplified to be

$$S_{\rm excl} = \sqrt{2[s - b\ \ln(1+s/b)]}. \tag{18}$$

We define the regions $S_{\rm excl} \leqslant 1.645$ as the regions that can be excluded at the 95% C.L.

Our 95% C.L. exclusion regions for the couplings ζ_1, ζ_2 for the unpolarized LBL scattering are shown in Figs. 6 and 7 with the cuts $|\eta_{\gamma\gamma}| < 2.5$, $m_{\gamma\gamma} > 1000$ GeV, for $\delta = 0$, $\delta = 5\%$, and $\delta = 10\%$. Note that for the unpolarized process the pure anomaly cross section is proportional to the coupling combination $48\zeta_1^2 + 40\zeta_1\zeta_2 + 11\zeta_2^2$ [65]. As a result, the exclusion regions are ellipses rotated counterclockwise in the plane (ζ_1, ζ_2) through the angle $0.5\arctan(80/37) \simeq 32.6°$ about the origin.

For the polarized LBL scattering at the CLIC, the exclusion bounds on the anomalous photon couplings are presented in Tables 2 and 3 using the cut $m_{\gamma\gamma} > 1000$ GeV. Note that the values of the expected integrated luminosities depend on the energy $\sqrt{s}$. As one can see from these tables, for both energies the exclusion bounds on couplings ζ_1 and ζ_2 weakly depend on the helicity of the initial electron beams.

Previously, the discovery potential for the LBL scattering at the 14 TeV LHC has been estimated in [63–65]. As was shown in [64], the 14 TeV LHC 95% C.L. exclusion limits on ζ_1 and ζ_2 couplings are 1.5×10^{-14} GeV^{-4} and 3.0×10^{-14} GeV^{-4}, respectively, for $L = 300$ fb^{-1} integrated luminosity. For $L = 3000$ fb^{-1} (HL-LHC), the values are twice smaller, 7.0×10^{-15} GeV^{-4} and 1.5×10^{-14} GeV^{-4}. The sensitivity in the (ζ_1, ζ_2) plane is shown in Fig. 8 taken from [65]. As one can see from Table 2, our CLIC bounds on the couplings ζ_1, ζ_2 for the LBL scattering with $\sqrt{s} = 1500$ GeV are comparable with the HL-LHC bounds [65]. However, for $\sqrt{s} = 3000$ GeV our lower bounds on ζ_1, ζ_2 are approximately one order of magnitude smaller than the HL-LHC ones, see Table 3.

In [43] the CLIC 95% C.L. sensitivity bounds on the coefficients f_{T_0}/Λ^4 and f_{T_9}/Λ^4 in the EFT Lagrangian (equivalent to the coefficients c_9/Λ^4 and c_{13}/Λ^4 in (3)) for $\sqrt{s} = 3000$ GeV and $L = 2000$ fb^{-1} are presented. Note

Table 2 The 95% C.L. exclusion limits on the couplings ζ_1 and ζ_2 for the CLIC collision energy $\sqrt{s} = 1500$ GeV, and the cut $m_{\gamma\gamma} > 1000$ GeV

Helicity		0	−0.8	0.8
Luminosity, fb^{-1}		2500	2000	500
$\lvert\zeta_1\rvert$, GeV^{-4} ($\zeta_2 = 0$)	$\delta = 0\%$	8.52×10^{-15}	7.35×10^{-15}	7.32×10^{-15}
	$\delta = 5\%$	9.84×10^{-15}	1.06×10^{-14}	9.59×10^{-15}
	$\delta = 10\%$	1.36×10^{-14}	1.42×10^{-14}	1.26×10^{-14}
$\lvert\zeta_2\rvert$, GeV^{-4} ($\zeta_1 = 0$)	$\delta = 0\%$	1.71×10^{-14}	1.45×10^{-14}	1.24×10^{-14}
	$\delta = 5\%$	2.06×10^{-14}	2.19×10^{-14}	2.01×10^{-14}
	$\delta = 10\%$	2.81×10^{-14}	2.95×10^{-14}	2.60×10^{-14}

Table 3 The same as in Table 2, but for $\sqrt{s} = 3000$ GeV

Helicity		0	−0.8	0.8
Luminosity, fb^{-1}		5000	4000	1000
$\lvert\zeta_1\rvert$, GeV^{-4} ($\zeta_2 = 0$)	$\delta = 0\%$	6.85×10^{-16}	8.82×10^{-16}	8.73×10^{-16}
	$\delta = 5\%$	1.90×10^{-15}	2.48×10^{-15}	1.56×10^{-15}
	$\delta = 10\%$	2.63×10^{-15}	3.37×10^{-15}	2.12×10^{-15}
$\lvert\zeta_2\rvert$, GeV^{-4} ($\zeta_1 = 0$)	$\delta = 0\%$	1.43×10^{-15}	1.85×10^{-15}	1.82×10^{-15}
	$\delta = 5\%$	3.99×10^{-15}	5.12×10^{-15}	3.28×10^{-15}
	$\delta = 10\%$	5.53×10^{-15}	7.10×10^{-15}	4.46×10^{-15}

that these coefficients are only parts of our couplings ζ_1 and ζ_2 (5). The bounds have been obtained by examining the anomalous quartic couplings of $ZZ\gamma\gamma$ vertex.

3 Conclusions

In the present paper, we have examined the anomalous quartic neutral couplings of the $\gamma\gamma\gamma\gamma$ vertex in the polarized light-by-light collisions of the Compton backscattered photons at the CLIC. Both the second and third stages of the CLIC are considered with the collision energies $\sqrt{s} = 1500$ GeV and $\sqrt{s} = 3000$ GeV, respectively. The helicity of the initial electron beam was taken to be $\lambda_e = \pm 0.8$. The unpolarized case ($\lambda_e = 0$) has been also considered. We used the $SU(2)_L \times U(1)_Y$ effective Lagrangian describing the contribution to the anomalous quartic neutral gauge boson couplings. Its part, relevant to the anomalous $\gamma\gamma\gamma\gamma$ vertex (4), expressed in terms of the physical fields, contains two couplings ζ_1, ζ_2 of dimension −4.

We have calculated both the differential and total cross sections of the light-by-light scattering $\gamma\gamma \to \gamma\gamma$, with the cut imposed on the rapidity of the final photons, $|\eta_{\gamma\gamma}| < 2.5$. The plots for two values of the collision energy $\sqrt{s}$ and three values of the electron beam helicity λ_e (including the unpolarized case) are presented. The anomaly and SM contributions to the cross sections are presented separately. The CLIC exclusion sensitivity bounds on the anomaly coupling constants ζ_1 and ζ_2, coming from the process $\gamma\gamma \to \gamma\gamma$, are calculated for three values of the systematic error, $\delta = 0\%$, $\delta = 5\%$, and $\delta = 10\%$. To reduce the SM background, we imposed the cut on the invariant mass of the outgoing photons, $m_{\gamma\gamma} > 1000$ GeV.

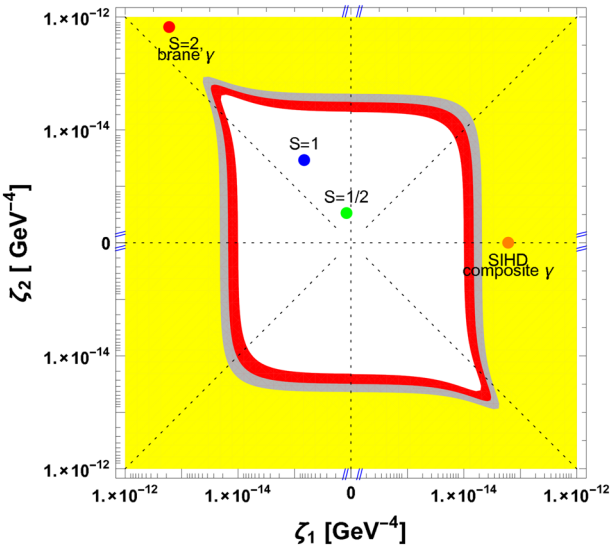

Fig. 8 The LHC sensitivity in the (ζ_1, ζ_2) plane. In particular, the red region can be probed at the 95% C.L. using proton tagging at the LHC. The white region is inaccessible. The figure is taken from Ref. [65]

For the unpolarized LBL scattering at the CLIC, the 95% C.L. exclusion regions are shown in Figs. 6 and 7. The exclusion bounds for the polarized LBL scattering are presented in Tables 2 and 3 for three values of the systematic error. For the e^+e^- collision energy $\sqrt{s} = 3000$ GeV, electron beam helicity $\lambda = 0.8$, and $\delta = 10\%$, our bounds on ζ_1, ζ_2 have appeared to be approximately one order of magnitude

stronger than the corresponding HL-LHC bounds obtained for $\sqrt{s} = 14$ TeV and integrated luminosity $L = 3000$ fb^{-1} in [65].

All said above allows us to conclude that the LBL scattering at the CLIC, especially the polarized, has a great physical potential in searching for the anomalous quartic neutral couplings of the $\gamma\gamma\gamma\gamma$ vertex.

Data Availability Statement This manuscript has no associated data or the data will not be deposited. [Authors' comment: No datasets were generated or analyzed during the current study.]

Funded by SCOAP[3].

References

1. W. Buchmuller, D. Wyler, Effective Lagrangian analysis of new interactions and flavour conservation. Nucl. Phys. B **268**, 621 (1986)
2. K. Hagiwara, R.D. Peccei, D. Zeppenfeld, K. Hikasa, Probing the weak boson sector in $e^+e^- \to W^+W^-$. Nucl. Phys. B **282**, 253 (1987)
3. S. Godfrey, Quartic gauge boson couplings, in Proceedings of the International Symposium on Vector Boson Self-Interactions, Los Angeles, CA, USA, 1–3 February 1995, pp. 209–223. arXiv:hep-ph/9505252
4. G. Balanger, F. Boudjema, $\gamma\gamma \to W^+W^-$ and $\gamma\gamma \to ZZ$ as tests of novel quartic couplings. Phys. Lett. B. **288**, 210 (1992)
5. W.J. Stirling, A. Werhenbach, Anomalous quartic couplings in $\nu\bar{\nu}\gamma\gamma$ production via WW-fusion at LEP2. Phys. Lett. B **466**, 369 (1999)
6. W.J. Stirling, A. Werhenbach, Anomalous quartic couplings in $W^+W^-\gamma$, $Z^0Z^0\gamma$ and $Z^0\gamma\gamma$ production at present and future e^+e^- colliders. Eur. Phys. J. C **14**, 103 (2000)
7. A. De Rújula, M.B. Gavela, P. Hernandez, E. Massó, The self-couplings of vector bosons: does LEP-1 obviate LET-2? Nucl. Phys. B **384**, 3 (1992)
8. K. Hagiwara, S. Ishihara, R. Szalapski, D. Zeppenfeld, Low-energy constraints on electroweak three gauge boson couplings. Phys. Lett. B **283**, 353 (1992)
9. K. Hagiwara, S. Ishihara, R. Szalapski, D. Zeppenfeld, Low energy effects of new interactions in the electroweak boson sector. Phys. Rev. D **48**, 2182 (1993)
10. C. Degrande et al., Effective field theory: a modern approach to anomalous couplings. Ann. Phys. **335**, 21 (2013)
11. O.J.P. Éboli, M.C. Gonzalez-Garcia, J.K. Mizukoshi, $pp \to jje^\pm\mu^\pm\nu\nu$ and $jje^\pm\mu^\mp\nu\nu$ at $\mathcal{O}(\alpha^6_{\rm em})$ and $\mathcal{O}(\alpha^{4\,2}_{\rm em})$ for the study of the quartic electroweak gauge boson vertex at CERN LHC. Phys. Rev. D **74**, 073005 (2006)
12. R.S. Gupta, Probing quartic gauge boson couplings using diffractive photon fusion at the LHC. Phys. Rev. D **85**, 014006 (2012)
13. S. Fichet, G. von Gersdorff, Anomolous gauge couplings from composite Higgs and warped extra dimensions. JHEP **03**, 102 (2014)
14. P. Achand et al. (L3 Collaboration), Study of the $W^+W^-\gamma$ process and limits on anomalous quartic gauge boson couplings at LEP. Phys. Lett. B **527**, 29 (2002)
15. A. Heister et al. (ALEPH Collaboration), Constraints on anomalous QGC's in e^+e^- interactions from 183 GeV to 239 GeV. Lett. B **602**, 31 (2004)
16. G. Abbiendi et al. (OPAL Collaboration), A study of $W^+W^-\gamma$ events at LEP. Phys. Lett. B **580**, 17 (2004)
17. J. Abdallah et al. (DELPHI Collaboration), Measurement of the $e^+e^- \to W^+W^-\gamma$ cross-section and limits on anomalous quartic gauge couplings with DELPHI. Eur. Phys. J. C **31**, 139 (2003)
18. G. Bélanger et al., Bosonic quartic couplings at LEP-2. Eur. Phys. J. C **13**, 283 (2000)
19. V.M. Abazov et al. (D0 Collaboration), Search for anomalous quartic $WW\gamma\gamma$ couplings in dielectron and missing energy final states in $\bar{p}p$ collisions at $\sqrt{s} = 1.96$ TeV. Phys. Rev. D **88**, 012005 (2013)
20. P. Achand et al. (L3 Collaboration), The $e^+e^- \to Z\gamma\gamma \to q\bar{q}\gamma\gamma$ reaction at LEP and constraints on anomalous quartic gauge boson couplings. Phys. Lett. B **540**, 43 (2002)
21. O.J.P. Éboli, M.C. Gonzalez-Garcia, S.M. Lietti, S.F. Novaes, Anomalous quartic gauge boson couplings at hadron colliders. Phys. Rev. D **63**, 075008 (2001)
22. O.J.P. Éboli, M.C. Gonzalez-Garcia, S.M. Lietti, Bosonic quartic couplings at CERN LHC. Phys. Rev. D **69**, 095005 (2004)
23. T. Pierzchała, K. Piotrzkowski, Sensitivity to anomalous quartic gauge couplings in photon–photon interactions at the LHC. Nucl. Phys. B. Proc. Suppl. **179**, 257 (2008)
24. E. Chapon, O. Kepka, C. Royon, Probing $WW\gamma\gamma$ and $ZZ\gamma\gamma$ quartic anomalous couplings with 10 pb^{-1} at the LHC. arXiv:0908.1061
25. E. Chapon, C. Royon, O. Kepka, Anomalous quartic $WW\gamma\gamma$, $ZZ\gamma\gamma$, and trilinear $WW\gamma$ couplings in two-photon processes at high luminosity at the LHC. Phys. Rev. D **81**, 074003 (2010)
26. A. Senol, Anomalous quartic $WW\gamma\gamma$ and $ZZ\gamma\gamma$ couplings in γp collision at the LHC. Int. J. Mod. Phys. A **29**, 1450148 (2014)
27. G. Perez, M. Sekulla, D. Zeppenfeld, Anomalous quartic gauge couplings and unitarization for the vector boson scattering process $pp \to W^+W^+jjX \to l^+\nu_l l^+\nu_l jjX$. Eur. Phys. J. C **78**, 759 (2018)
28. Y.-C. Guo, Y.-Y. Wang, J.-C. Yang, C.-X. Yue, Constraints on anomalous quartic gauge couplings via $W\gamma jj$ production at the LHC. Chin. Phys. C **44**, 123105 (2020)
29. S. Tizchang, S.M. Etesami, Pinning down the gauge boson couplings in $WW\gamma$ production using forward proton tagging. JHEP **07**, 191 (2020)
30. J.-W. Zhu, R.-Y. Zhang, W.-G. Ma, Q. Yang, Y. Jiang, $W^+W^-\gamma$ production at hadron colliders with NLO QCD+EW corrections and parton shower effects. J. Phys. G Nucl. Part. Phys. **47**, 055006 (2020)
31. İ. Şahin, B. Şahin, Anomalous quartic $ZZ\gamma\gamma$ couplings in gamma-proton collision at the LHC. Phys. Rev. D **86**, 115001 (2012)
32. A.M. Sirunyuan et al. (CMS Collaboration), Measurement of the cross section for electroweak production of a Z boson, a photon and two jets in proton-proton collisions at $\sqrt{s} = 13$ TeV and constraints on anomalous quartic couplins. JHEP **06**, 076 (2020)
33. G. Aad et al. (ATLAS Collaboration), Measurements of $Z\gamma$ and $Z\gamma\gamma$ production in pp collisions at $\sqrt{s} = 8$ TeV with the ATLAS detector. Phys. Rev. D **93**, 112002 (2006)
34. V. Ari, A. Gutiérrez-Rodriguez, M.A. Hernandez-Ruiz, M. Köksal, Anomalous quartic $W^+W^-\gamma\gamma$ couplings in e^-p collisions at the LHeC and the FCC-he. Eur. Phys. J. Plus **135**, 336 (2020)

35. V. Ari, E. Gurkanli, A.A. Billur, M. Köksal, Model independent study for the anomalous quartic $WW\gamma\gamma$ couplings at future electron-proton colliders. Nucl. Phys. B **957**, 115102 (2020)
36. A. Gutierrez-Rodriguez, M.A. Hernandez-Ruiz, E. Gurkanli, V. Ari, M. Köksal, Study on the anomalous quartic $W^+W^-\gamma\gamma$ couplings of electroweak bosons in e^-p collisions at the LHeC and the FCC-he. Eur. Phys. J. C **81**, 210 (2021)
37. A. Denner, S. Dittmaier, M. Roth, D. Wackeroth, Probing anomalous quartic gauge-boson couplings via $e^+e^- \to 4$ fermions + γ. Eur. Phys. J. C **20**, 201 (2001)
38. O.J.P. Éboli, M.C. Gonzalez-Garcia, S.F. Novaes, Quartic anomalous couplings in $e\gamma$ colliders. Nucl. Phys. B **411**, 381 (1994)
39. S. Atağ, İ. Şahin, Anomalous quartic $WW\gamma\gamma$ and $ZZ\gamma\gamma$ couplings in $e\gamma$ collision with initial beams and final state polarizations. Phys. Rev. D **75**, 073003 (2007)
40. O.J.P. Éboli, J.K. Mizukoshi, Probing anomalous quartic couplings in $e\gamma$ and $\gamma\gamma$ colliders. Phys. Rev. D **64**, 075011 (2001)
41. İ. Şahin, Anomalous quartic $WW\gamma\gamma$ and $WWZ\gamma$ couplings through W^+W^-Z production in $\gamma\gamma$ collisions. J. Phys. G Nucl. Part. Phys. **36**, 075007 (2009)
42. M. Köksal, Anomalous quartic $ZZ\gamma\gamma$ couplings at the CLIC. Eur. Phys. J. Plus **130**, 75 (2015)
43. M. Köksal, V. Ari, A. Senol, Search for anomalous quartic $ZZ\gamma\gamma$ couplings in photon-photon collisions. Adv. High Energy Phys. **2016**, 8672391 (2016)
44. H. Braun et al. (CLIC Study Team), CLIC 2008 parameters, CERN-OPEN-2008-021, CLIC-NOTE-764
45. M.J. Boland et al. (CLIC and CLICdp Collaborations), Updated baseline for a staged Compact Linear Collider, CERN-2016-004. arXiv:1608.07537
46. D. Dannheim et al., CLIC e^+e^- Linear collider studies, in Proceedings of 2013 Community Summer Study on the Future of U.S. Particle Physics: Snowmass on the Mississippi (CSS2013), 29 July–6 August, 2013, MN, USA. arXiv:1208.1402
47. J. de Blas et al. (eds.), The CLIC Potential for New Physics, CERN Yellow report: Monographs, Vol. 3/2018, CERN-2018-009-M (CERN, Geneva, 2018)
48. R. Franceschini, Beyond the Standard Model physics at CLIC. Int. J. Mod. Phys. A **35**, 2041015 (2020)
49. M. Aaboud et al. (ATLAS Collaboration), Evidence for light-by-light scattering in heavy-ion collisions with the ATLAS detector at the LHC. Nat. Phys. **13**, 852 (2017)
50. G. Aad et al. (ATLAS Collaboration), Observation of light-by-light scattering in ultraperipheral Pb + Pb collisions with the ATLAS detector. Phys. Rev. Lett. **123**, 052001 (2019)
51. D. d'Enterria et al. (CMS Collaboration), Evidence for light-by-light scattering in ultraperipheral PbPb collisions at $\sqrt{s}$ =5.02 TeV. Nucl. Phys. A **982**, 791 (2019)
52. S. Atağ, S.C. İnan, İ. Şahin, Extra dimensions in $\gamma\gamma \to \gamma\gamma$ process at the CERN-LHC. JHEP **09**, 042 (2010)
53. S.C. İnan, A.V. Kisselev, Probe of the Randall–Sundrum-like model with the small curvature via light-by-light scattering at the LHC. Phys. Rev. D **100**, 095004 (2019)
54. S.C. İnan, A.V. Kisselev, A search for axion-like particles in light-by-light scattering at the CLIC. JHEP **06**, 183 (2020)
55. S.C. İnan, A.V. Kisselev, Polarized light-by-light scattering at the CLIC induced by axion-like-particles. Chin. Phys. C **45**, 043109 (2021)
56. I.F. Ginzburg, G.L. Kotkin, V.G. Serbo, V.I. Telnov, Colliding γe and $\gamma\gamma$ beams based on the single-pass e^+e^- colliders (of VLEPP Type). Nucl. Instrum. Methods **205**, 47 (1983)
57. I.F. Ginzburg, G.L. Kotkin, S.L. Panfil, V.G. Serbo, V.I. Telnov, Colliding γe and $\gamma\gamma$ beams based on single-pass e^+e^- accelerators II. Polarization effects, monochromatization improvement. Nucl. Instrum. Methods Phys. Res. **219**, 5 (1984)
58. O. Çakir, K.O. Ozansoy, Unparticle searches through gamma-gamma scattering. Eur. Phys. J. C **56**, 279 (2008)
59. G.A. Moortgat-Pick et al., The role of polarised positrons and electrons in revealing fundamental interactions at the Linear Collider. Phys. Rep. **460**, 131 (2008)
60. R. Franceschini, P. Roloff, U. Schnoor, A. Wulzer, The compact linear e^+e^- collider (CLIC): physics potential. arXiv:1812.07986
61. E. da Silva Almeida, O.J.P. Éboly, M.C. Gonzalez-Garcia, Unitarity constraints on anomalous quartic couplings. Phys. Rev. D **101**, 113003 (2020)
62. Y.-J. Zhang, J.-F. Shen, Probing anomalous tqh couplings via single top production in associated with the Higgs boson at the HE-LHC and FCC-hh. Eur. Phys. J. C **80**, 811 (2020)
63. D. d'Enterria, G.G. da Silveira, Observing light-by-light scattering at the Large Hadron Collider. Phys. Rev. Lett. **111**, 080405 (2013) [Erratum, Phys. Rev. Lett. **116**, 129901 (2016)]
64. S. Fichet et al., Probing new physics in diphoton production with proton tagging at the Large Hadron Collider. Phys. Rev. D **89**, 114004 (2014)
65. S. Fichet, Light-by-light scattering with intact protons at the LHC: from standard model to new physics. JHEP **02**, 165 (2015)